

## Project Note

# DVRK force sensor calibration

---

## Introduction

An accurate force sensor is an essential foundation for robotic tactile perception. In the previous stiffness estimation experiment<sup>1</sup>, our calibrated Mat6 force sensor shows ability to classify three objects of different shore D hardness (HD13, HD30, HD90). However, the large size of the Mat6 force sensor makes it impractical when touching small objects. Besides, its large size causes large contact area with the target objects, which brings much shear force during the contact process. Therefore, the force value measurement will be very inaccurate.

In order to perceive smaller objects and obtain more accurate force measurement, **DVRK force sensor** is more suitable for our tactile perception task because of its smaller size. For any kind of sensor, **calibration** is an inevitable step before using it.

In contrast to the calibration of Mat6 force sensor, a more convenient UR5 movement method is implemented for the calibration of Mat6 force sensor. By **adding a force sensor frame** which is the child frame of end effector frame, the pose of the end effector could be computed according to the transform between these two frames.

## Methods

### Setup

#### ➤ UR5 robot arm

By attaching the force sensor to the end effector of UR5 robot arm, we could let DVRK force sensor contact loadstar/ATI with specific orientations by controlling the position and orientation of the end effector of UR5 robot arm.

#### ➤ DVRK force sensor

Some hardware preparations are necessary before calibration. In details, the following

---

<sup>1</sup>[https://docs.google.com/document/d/17t4pxZcHTLGggsyB38sd3BSYl8o4NnqVZlId\\_\\_ppN8Y/edit?usp=s](https://docs.google.com/document/d/17t4pxZcHTLGggsyB38sd3BSYl8o4NnqVZlId__ppN8Y/edit?usp=s)haring

two things should be done:

- We should make sure the sensors in the DVRK force sensor could measure the magnetic field values successfully.
  - The DVRK force sensor could be attached to the UR5 robot stably. (Finished 9.9 - 9.15)
- Loadstar / ATI

An Loadstar or ATI could help us obtain ground truth force values.

## Procedure

1. Control the **movement of the UR5 robot arm** so that the force sensor contacts the loadstar in specific poses. And then **collect** magnetic sensor values (from DVRK force sensor) and force values (from loadstar) during contact process.
2. Train a regression model between magnetic sensor values and force values.
3. Give an unknown contact to the force sensor, use the trained regression model to predict force value from magnetic sensor values.

## Implement

### UR5 robot arm simulation (Finished 9.16 - 9.21)

A force sensor frame “my\_force\_sensor\_link” is defined to directly control the pose of force sensor. The movement of UR5 robot robot arm could be computed by transforming the pose of force sensor to the

pose of the end effector.

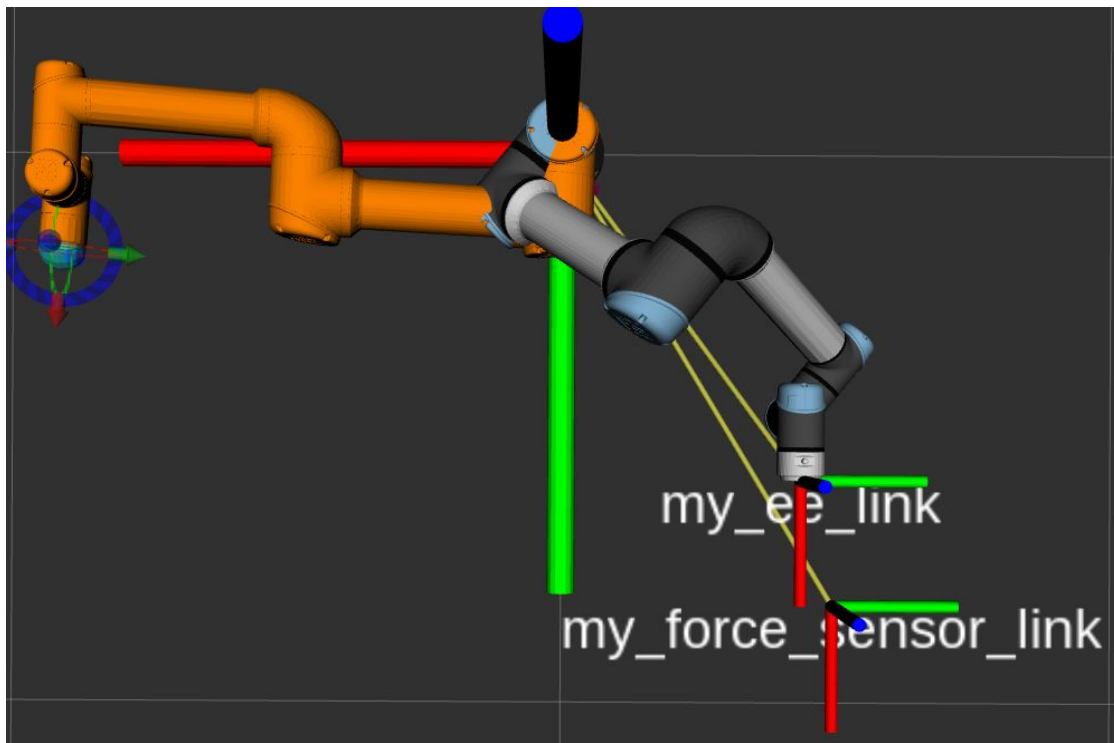


Figure 1: Two frames defined in the calibration implement.

After letting the DVRK force sensor touch the Loadstar/ATI with several orientations, the force sensor's trajectory (green line) shows **force sensor always moves in the same vertical path.**

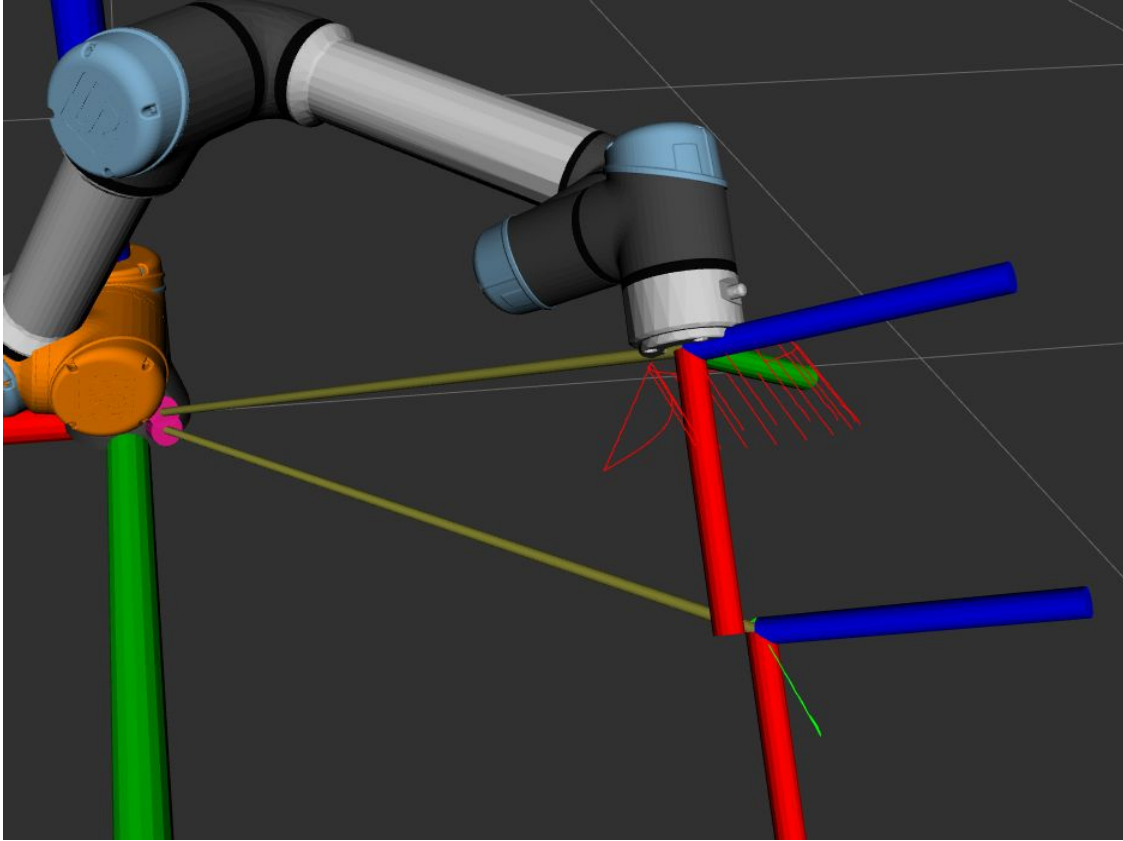


Figure 2: Trajectory of force sensor and end effector

## Transformation (Finished 9.23 - 9.29)

### Purpose

The working mechanism of DVRK force sensor (or Mat6 force sensor) is that there are three magnetic sensors inside the force sensor, and the magnetic field values measured by these three sensors vary with the deformation of the DVRK force sensor when a force is imposed on. Therefore, we hope to calculate a regression model between the magnetic field values and the force values and this model could accurately output any force (which should be a three-dimensional vector) imposed on DVRK.

## 3D rigid registration of magnetic field data (Finished 9.23 - 9.29)

### Purpose

The working mechanism of DVRK force sensor (or Mat6 force sensor) is that there are three magnetic sensors inside the force sensor, and the magnetic field values measured by these three sensors vary with the deformation of the DVRK force sensor when a force is imposed on. Therefore, we hope to calculate a regression model between the magnetic field values and the force values and this model could accurately output any force (which should be a three-dimensional vector) imposed on DVRK.

However, the tiny space inside DVRK force sensor determines the orientations of three sensors are not consistent. And thus, their measured magnetic field values are not comparable. In order to utilize the magnetic field values of all these three sensors, the first thing we need to do is to align the measured magnetic field data in the same coordinate system.

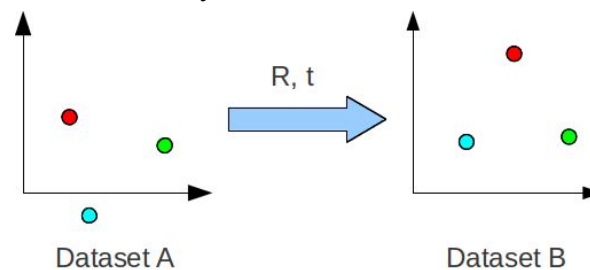


Figure 3: Example of three-dimensional registration between two datasets.

### Procedure

Firstly, I collected the magnetic field values of these three sensors without attaching the magnet. This step is to make sure we have collected enough data so as to estimate the linear correlation of these three sensors.

Our goal is to compute the optimal transform between two three-dimensional datasets. We have three matrices  $Mag_1, Mag_2, Mag_3$  which represent the raw magnetic data collected without any force imposed on DVRK.

This problem is to solve  $R, t$  from this equation, where  $R, t$  are the transforms applied to matrix  $Mag_2$  to align it with dataset  $Mag_1$ , as best as possible.

$$Mag_1 = R * Mag_2 + t$$

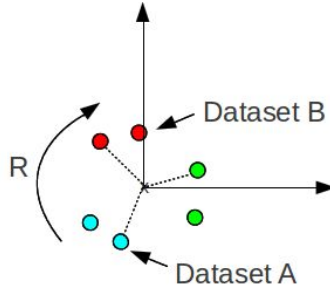


Fig 4: 3D Rigid registration

A Singular value decomposition (SVD) based 3D rigid registration method<sup>2</sup> is used to calculate the optimal transform between dataset  $Mag_2$  and dataset  $Mag_1$ .

1. Find the centroids of these two datasets.
2. Bring both dataset into origin and find the optimal rotation.

$$H = \sum (Mag_1^i - Centroid(Mag_1))(Mag_2^i - Centroid(Mag_2))^T$$

$$[U, S, V] = SVD(H)$$

$$R = VU^T$$

3. Find the translation.

Result

Registration result of magnetic field values collected without any force (three axes).

---

<sup>2</sup> “Least-Squares Fitting of Two 3-D Point Sets”, Arun, K. S. and Huang, T. S. and Blostein, S. D, IEEE Transactions on Pattern Analysis and Machine Intelligence, Volume 9 Issue 5, May 1987

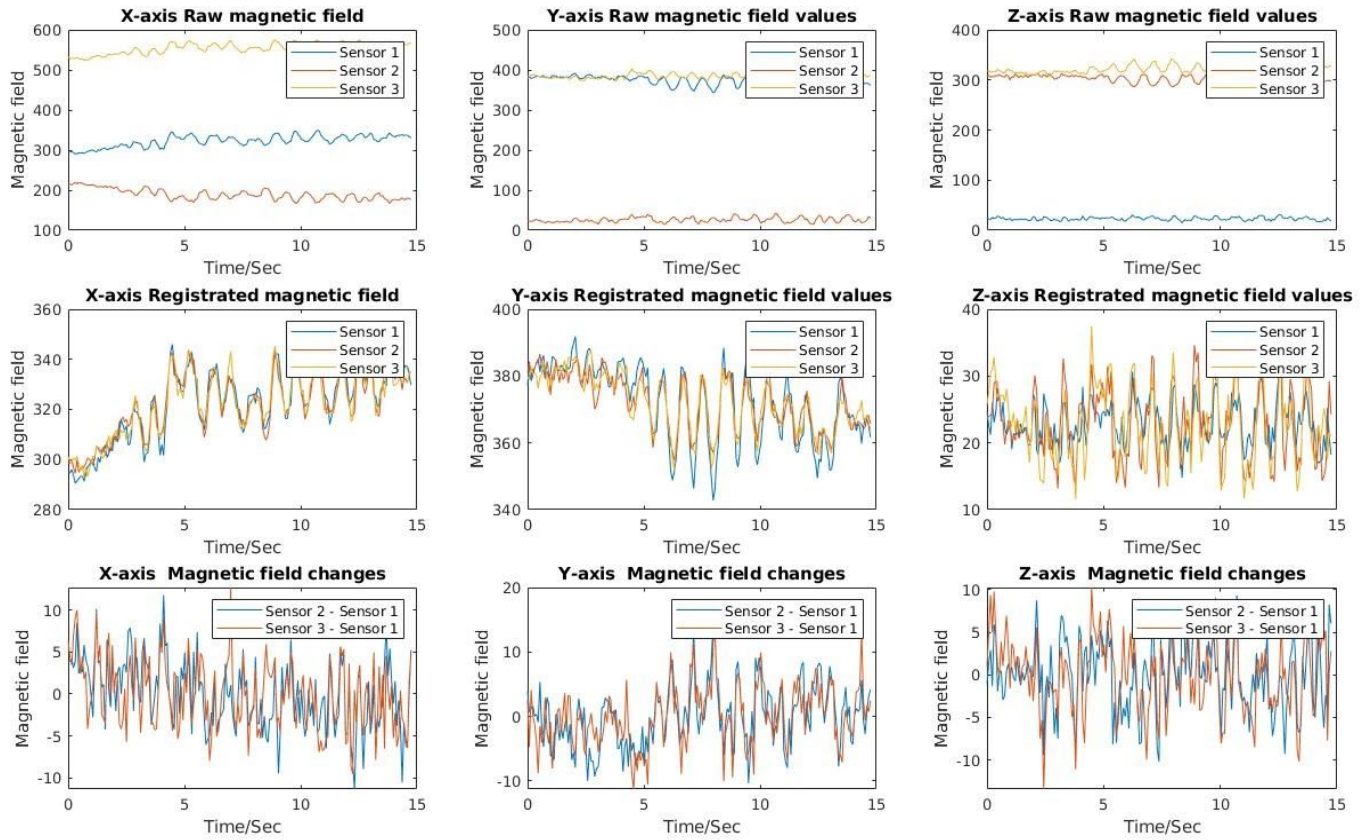


Fig 5: Registration result of magnetic field data without any force imposed on DVRK

The above figure shows raw magnetic field values, registered magnetic field values and the changes of magnetic field values between different sensors in x, y and z-axis. The registered magnetic field values of the three sensors are comparable in all axis, which confirms the plausibility of calculated transforms.

## Experiment of contacting loadstar with different orientations(Finished 9.23 - 10.6)

### UR5 Setup

According to previous calibration plan, the magnetic data and ground truth force data need to be collected when the force sensor touches Loadstar / ATI with different orientations. For our Mat6 force sensor, the range of theta is  $0 - 2\pi$ , and the range of phi is  $0 - \pi / 4$ .

But for DVRK force sensor, I found that letting the force sensor contact Loadstar/ATI with these various orientations is impractical. Because the DVRK force sensor has a long body and the movement of end-effector is likely to cause collision between DVRK force sensor and the wrist/shoulder of UR5 robot arm. Therefore, in the first experiment, I collected data with theta in  $[\pi/4, 5\pi/4]$  and phi in  $[0, \pi/12]$ .

Since these data are collected with a few orientations, it could be used to train a force regression model, or to validate the performance of later force regression model.

### Registration result of magnetic field values<sup>3</sup>

The raw magnetic field values need to be registered since the three sensors are not in the same frame. According to the transforms calculated from magnetic field data without any force, the registered magnetic field values could be obtained. The following figure shows raw data, registered magnetic field data and changes of magnetic field values in x, y and z axis.

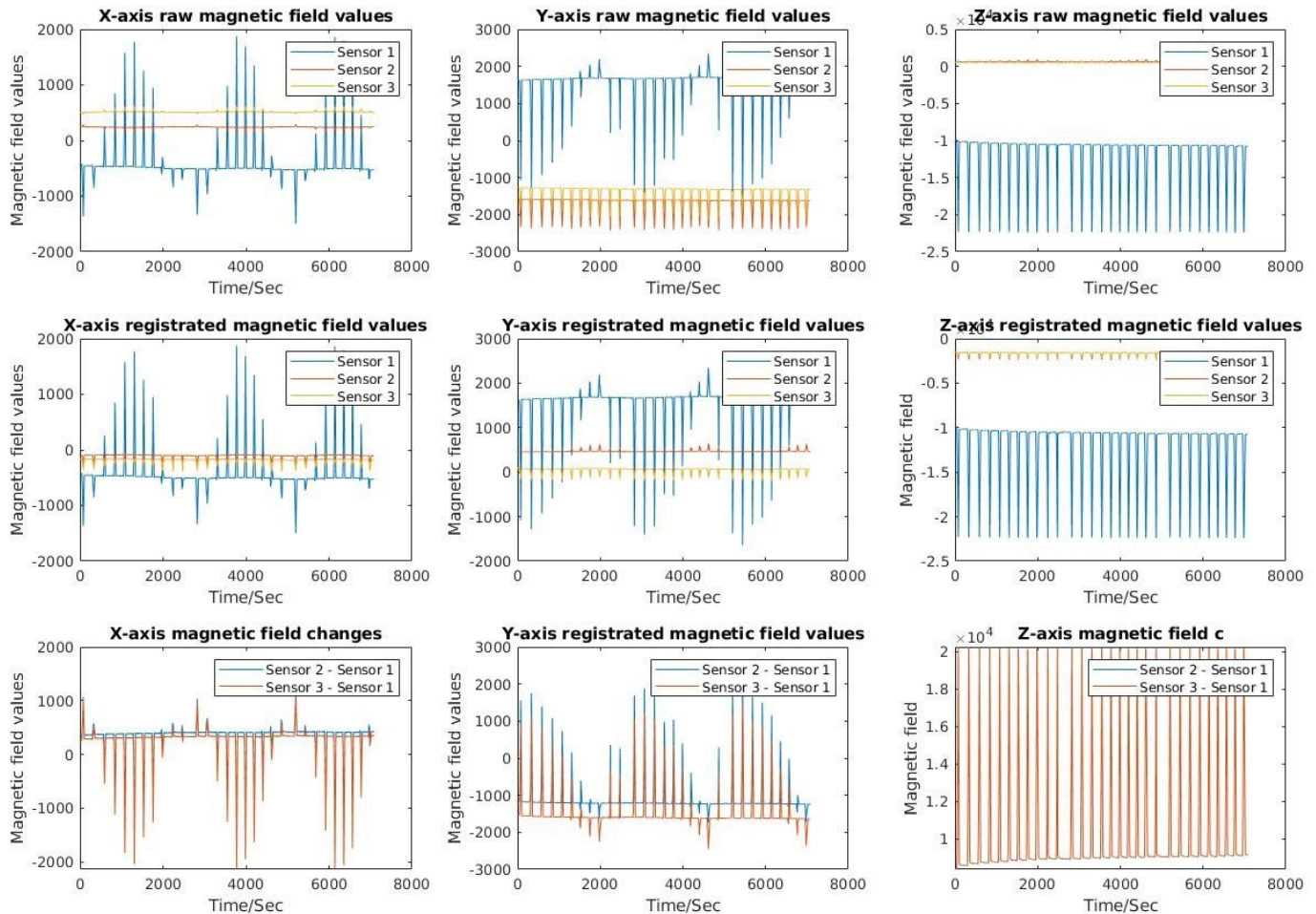


Fig 6: Registration result of magnetic field data

### Feature extraction

According to the design of DVRK force sensor, the changes of registered magnetic field values between different sensor reflects the magnetic changes caused by force imposed on DVRK.

<sup>3</sup> [https://nghiaho.com/?page\\_id=671](https://nghiaho.com/?page_id=671)



But according to the above figure, the changes of magnetic field values between sensor 2 and sensor 1 is **highly correlated** to the changes of magnetic field values between sensor 3 and sensor 1. Therefore, the original six-dimensional feature should contain a lot of redundant information.

The following table shows the correlation coefficients between different features:

Correlation coefficient	Mag_21_x	Mag_21_y	Mag_21_z	Mag_31_x	Mag_31_y	Mag_31_z
Mag_21_x	1.0000	-0.3813	-0.6143	0.9995	-0.3049	-0.6137
Mag_21_y	-0.3813	1.0000	0.6865	-0.3709	0.9890	0.6919
Mag_21_z	-0.6143	0.6865	1.0000	-0.6220	0.5725	1.0000
Mag_31_x	0.9995	-0.3709	-0.6220	1.0000	-0.2915	-0.6212
Mag_31_y	-0.3049	0.9890	0.5725	-0.2915	1.0000	0.5786
Mag_31_z	-0.6137	0.6919	1.0000	-0.6212	0.5786	1.0000

Tab 1: correlation coefficients between different features

The following heatmap shows the visualization of correlation matrix between these six features:

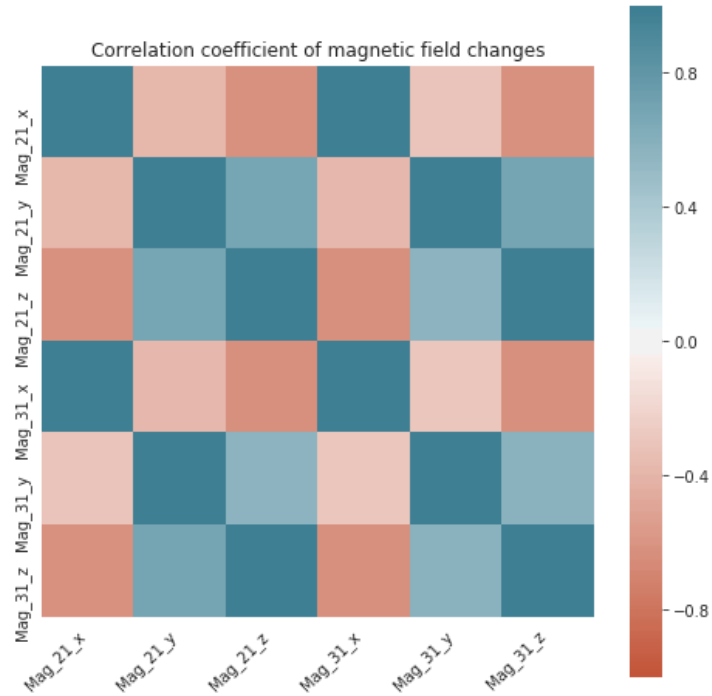


Fig 7: Heatmap of correlation coefficients between different features

The above analysis verifies our assumption that the six-dimensional feature contains redundant information. Especially, the correlation coefficients between Mag\_21\_x and Mag\_31\_x, Mag\_21\_y and Mag\_31\_y, Mag\_21\_z and Mag\_31\_z are close to 1. Therefore, principal component analysis (PCA) is used to reduce the dimension of different data.

After using PCA to reduce dimension, the following table and figure shows the variance ratio of all principal components:

Principal Components Number	1	2	3	4	5	6
Variance Ratio	98.3901%	1.0102%	0.5993%	0.0002%	0.0001%	0.0001%

Tab 2: Variance ratio of PCA

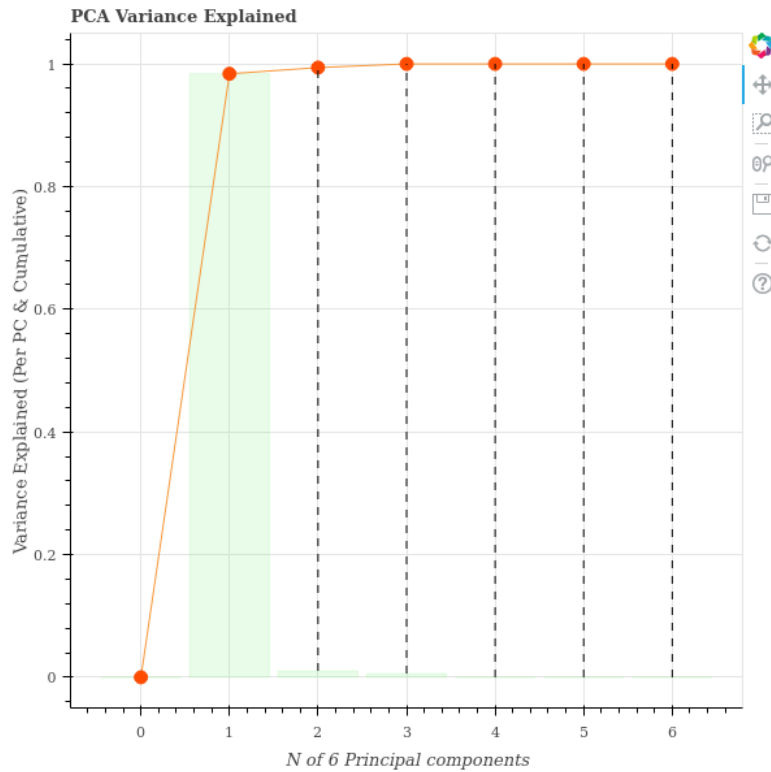


Fig 8: PCA variance explained analysis

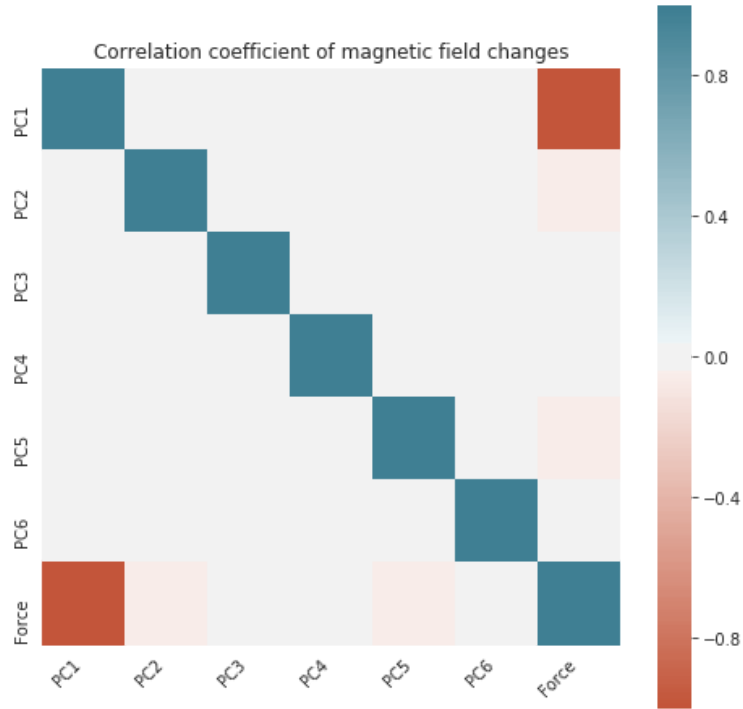


Fig 9: Heatmap of correlation coefficients between normal force and principal components

According to the above figure, the first principal component could represent about **98%** of the variance of the original six-dimensional feature. Also, the correlation coefficient between normal force and the first principal component is **-0.9921**.

Therefore, we choose the first principal component as the feature and calculate a regression model between the first principal component and normal force.

Calculate a regression model to predict normal force

According to the observation, the relationship between feature and normal force is very close to a polynomial curve. The following three figures show the regression result of third-order polynomial regression, fourth-order polynomial regression and fifth-order polynomial regression.

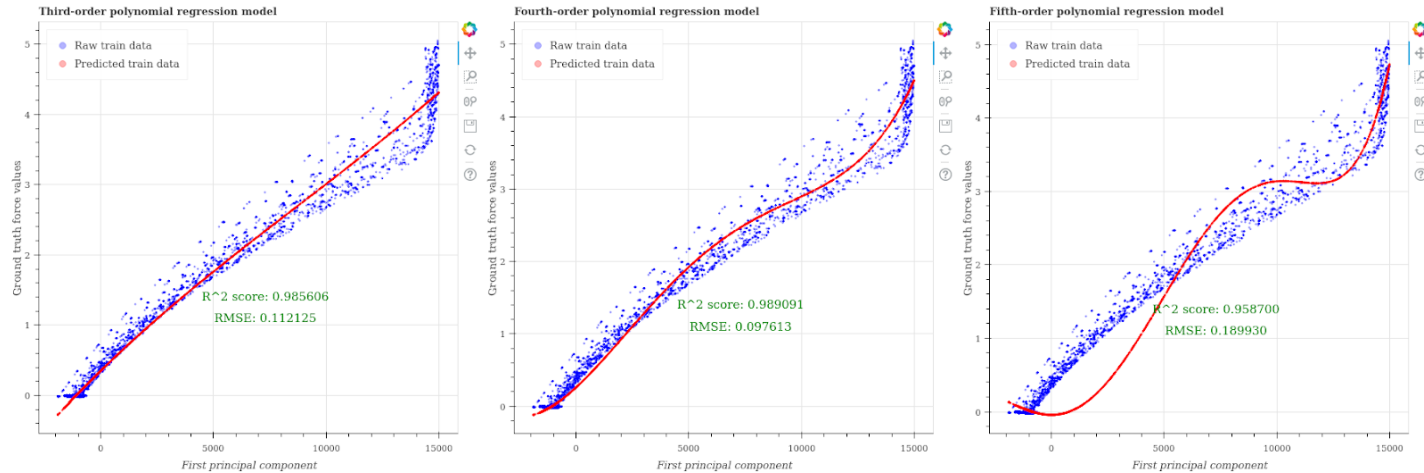


Fig 10: Polynomial regression model of normal force

It is obvious that the fourth-order regression model best fits the relationship between a feature and normal force. Also, the following table shows the RMSE and  $R_2$  score between ground truth normal force and predicted normal force. The result also shows that the prediction result of the fourth-order regression model produces the lowest error.

	Third order	Fourth order	Fifth order
RMSE	0.1121	0.0976	0.1899
$R_2$ score	0.9856	0.9891	0.9587

Tab 3: Prediction error analysis

## Experiment of shear calibration based on ATI

### UR5 Setup

To figure out the limited orientations of DVRK force sensor, shear based calibration could make sure the ATI contacts force sensor with different positions. When the force sensor contacts ATI in the normal direction with a small force, the small movement in horizontal plane could cause shear contact of the force sensor. Since the tip of DVRK force sensor is deformable, this kind of shear contact could make sure the contact area cover different position of force sensor's tip.

3D rigid registration<sup>4</sup> (Finished 9.29 - 10.06)

The three sensors inside DVRK are measuring the same magnetic field, so the first thing is to find optimal rotation and translation between these two point sets.

<sup>4</sup> [https://nghiaho.com/?page\\_id=671](https://nghiaho.com/?page_id=671)

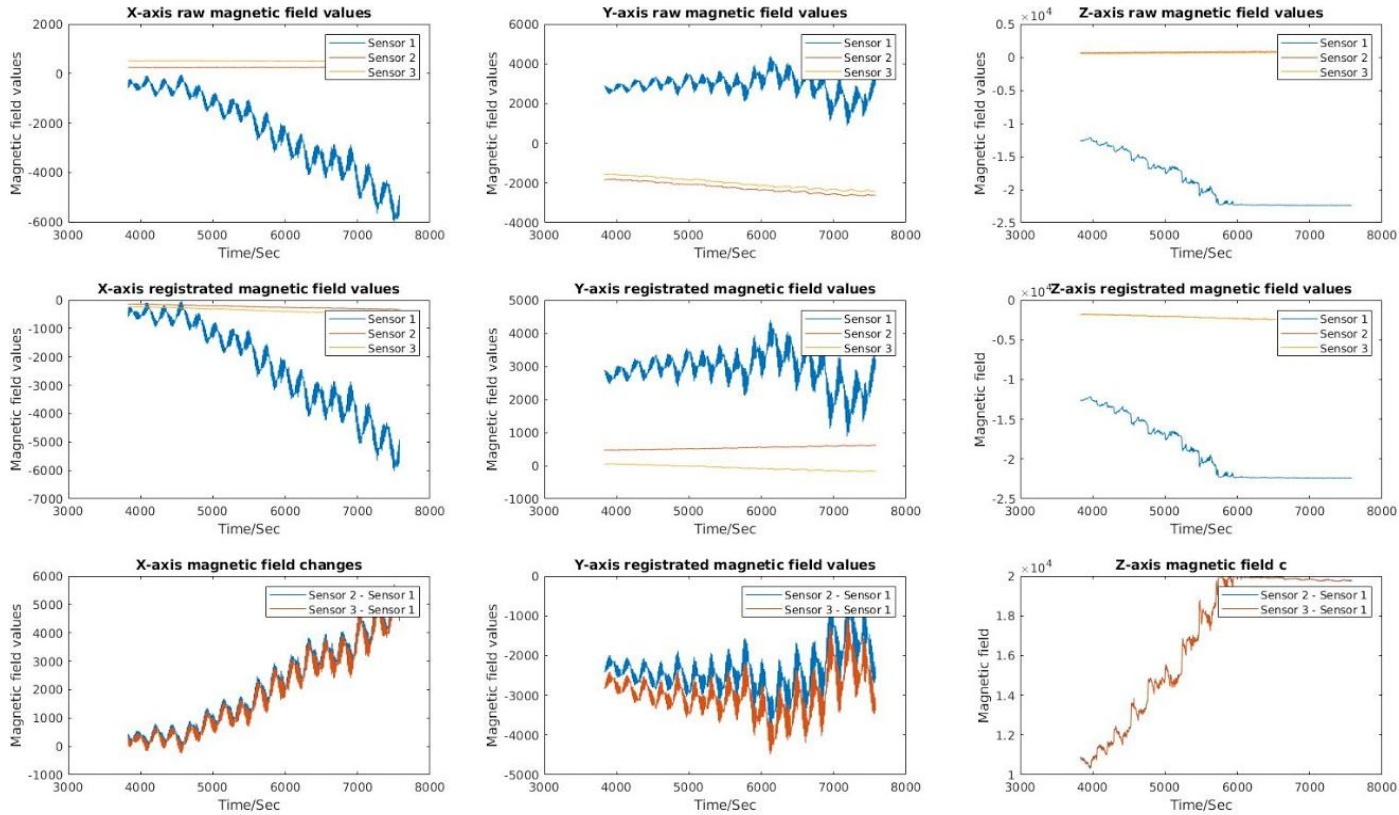


Fig 11: Registration result of magnetic field data

Feature extraction(**Finished 9.29 - 10.06**)

Similar to the previous experiment, principal component analysis (PCA) is used to reduce the dimension of features and extract the principal component with the largest variance.

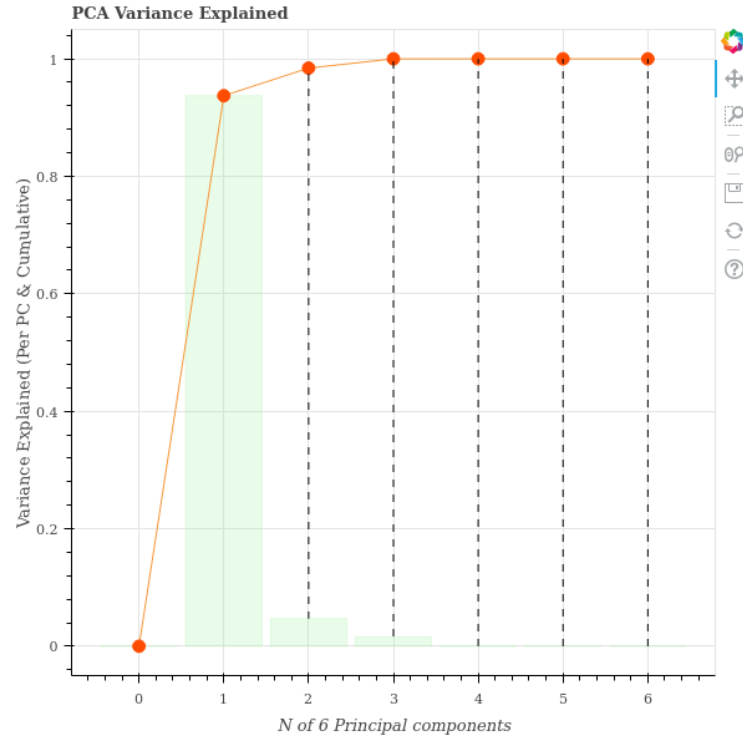


Fig 12: PCA variance explained analysis (shear data)

The correlation coefficients between different principal components and force in x, y and z direction are calculated<sup>5</sup>.

<sup>5</sup> Aquilina, K., Barton, D. A., & Lepora, N. F. (2019). Shear-invariant Sliding Contact Perception with a Soft Tactile Sensor. arXiv preprint arXiv:1905.00842.

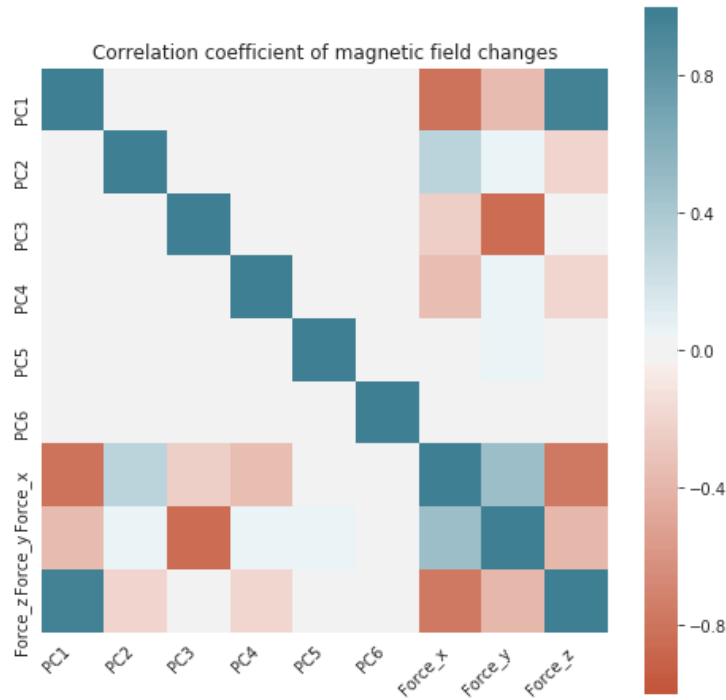


Fig 13: Heatmap of correlation coefficients between principal components and force

	Force_x	Force_y	Force_z
PC1	-0.8102	-0.3649	0.9534
PC2	0.3189	0.0560	-0.2039
PC3	-0.2320	-0.8528	0.0046
PC4	-0.3433	0.0606	-0.2006

Tab 4: Correlation coefficients between principal components and force

According to the above analysis, the first principal component shows high correlation coefficient with Force\_x and Force\_z, and the third principal component shows high correlation coefficient with Force\_y.

Normal force Regression(Finished 9.29 - 10.06)

The following figure shows regression results between the first principal component and force in the z-axis. It verifies that fourth-order regression model is better than third-order regression model and fifth-order regression model.

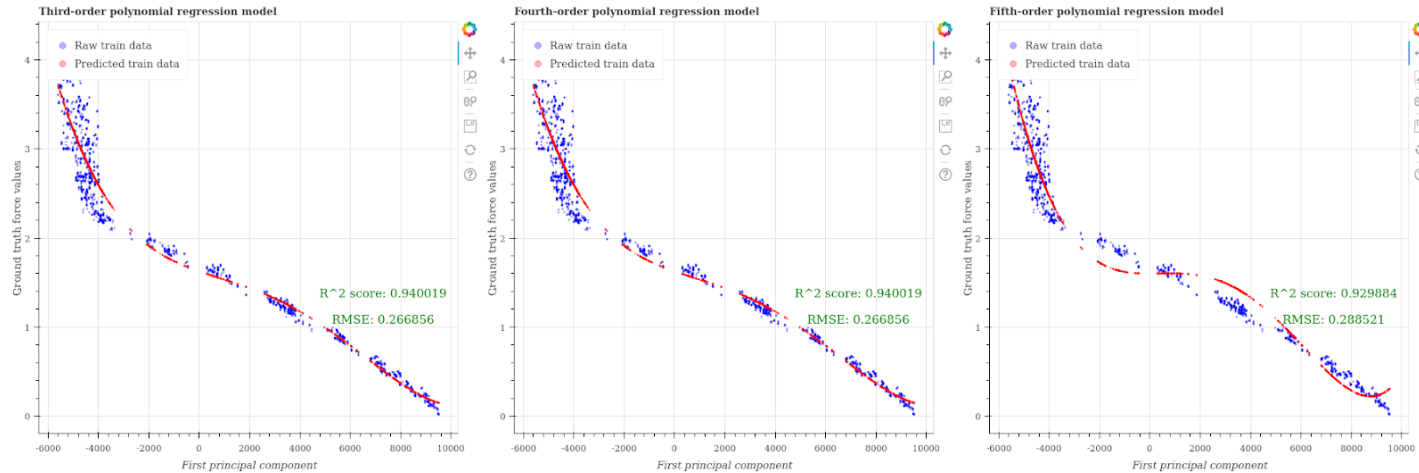


Fig 14: Polynomial regression model of normal force

For the regression model of force in the x-axis and y-axis, since current data are only collected with a shear distance of 0.005, the number of data points is not enough to compute an accurate regression model. In other words, **a longer sliding distance** is needed when collecting the data.

## Shear force Regression

Shear data collection(**Finished 10.06 - 10.13**)

In the previous method, force data and magnetic data are collected after the movement of UR5, so the data of sliding process is not collected. I added one data collection part which is used to collect data when the sliding occurs.

In detail:

1. Subscribe topics of magnetic field values, ati force data,
2. Call a rosservice which tells ros node to start collecting data.
3. Call a rosservice which tells ros node to stop collecting data.

Force data transformation(**Finished 10.06 - 10.13**)

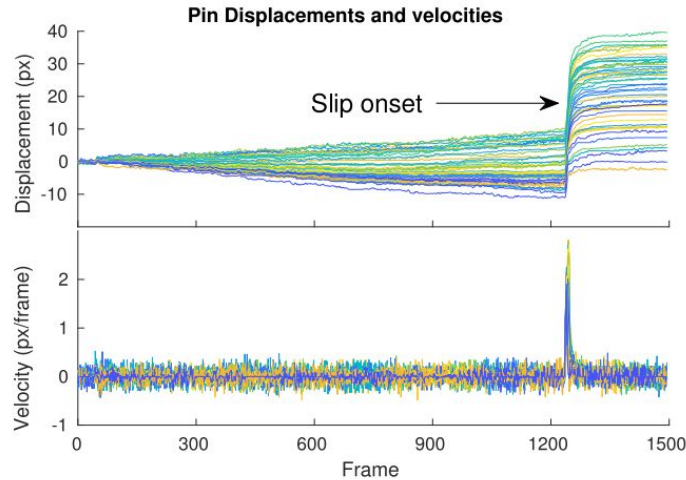
Transform ati force data from ati frame to world frame.

## Literature review:

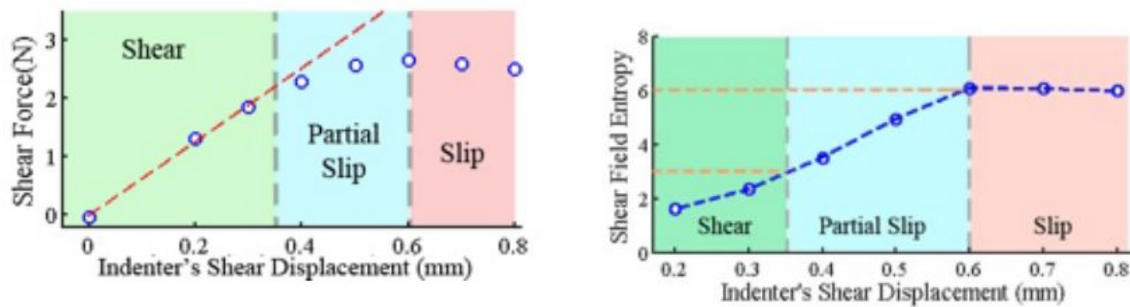
This paper proposed a method of detecting slip with a biomimetic optical tactile sensor --- the TacTip sensor, which operates by measuring the positions of internal pins embedded in its compliant skin. According to the experiment, the **velocity** of the movement of pins could discriminate the static and slip of this sensor. As a conclusion, an **SVM** applied to pin velocities from the TacTip optical tactile sensor is a robust method to detect slip.<sup>6</sup>

<sup>6</sup> James, J. W., Pestell, N., & Lepora, N. F. (2018). Slip detection with a biomimetic tactile sensor. IEEE Robotics and Automation Letters, 3(4), 3340-3346.





This paper presented a method of sensing the normal, shear and torsional load on the contact surface with a GelSight tactile sensor. The analysis of the sequence of images under the external load shows that their deformation could indicate the conditions of contact. As a statistical representation, the entropy which reflects the inhomogeneity of the displacement field magnitude shows the degree of the partial slip or slip quite well<sup>7</sup>.



Shear displacement vs Shear force

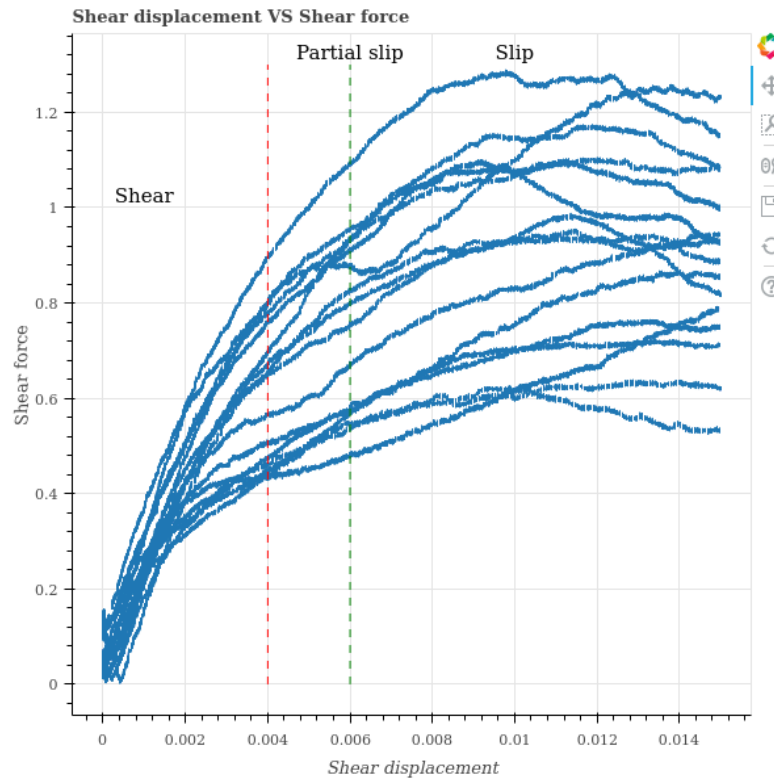
#### Contact state classification (Finished 10.14 - 10.20)

The states under shear load can be divided into the shear state, the partial slip state and the slip state according to the relative displacement between the sensor and the contact surface.

1. The shear state: when the shear load is small and no relative movement occurs between the sensor and contact region.
2. The partial slip state: when the shear load is larger and relative movement occurs in part of the contact region.
3. The slip state: when the shear load is very large and there is relative movement over the whole contact region.

<sup>7</sup> Yuan, W., Li, R., Srinivasan, M. A., & Adelson, E. H. (2015, May). Measurement of shear and slip with a GelSight tactile sensor. In 2015 IEEE International Conference on Robotics and Automation (ICRA) (pp. 304-311). IEEE.

The analysis of the relationship between shear displacement and shear force on DVRK force sensor is shown in the following figure:



In order to divide the contact states into shear state, partial slip state and slip state, I set the displacement thresholds manually. In the shear state, the shear force should be linearly increasing with the shear displacement. And in the slip state, the shear force should keep a nearly constant value with the increase of shear displacement.

Shear force regression (Finished 10.14 - 10.20)

-----  
Shear force is the force in the tangential direction on the contact surface.

	RMSE of test set	R <sup>2</sup> of test set	
X axis	0.068261	0.985863	
Y axis	0.041712	0.995738	
Z axis	0.030135	0.995519	

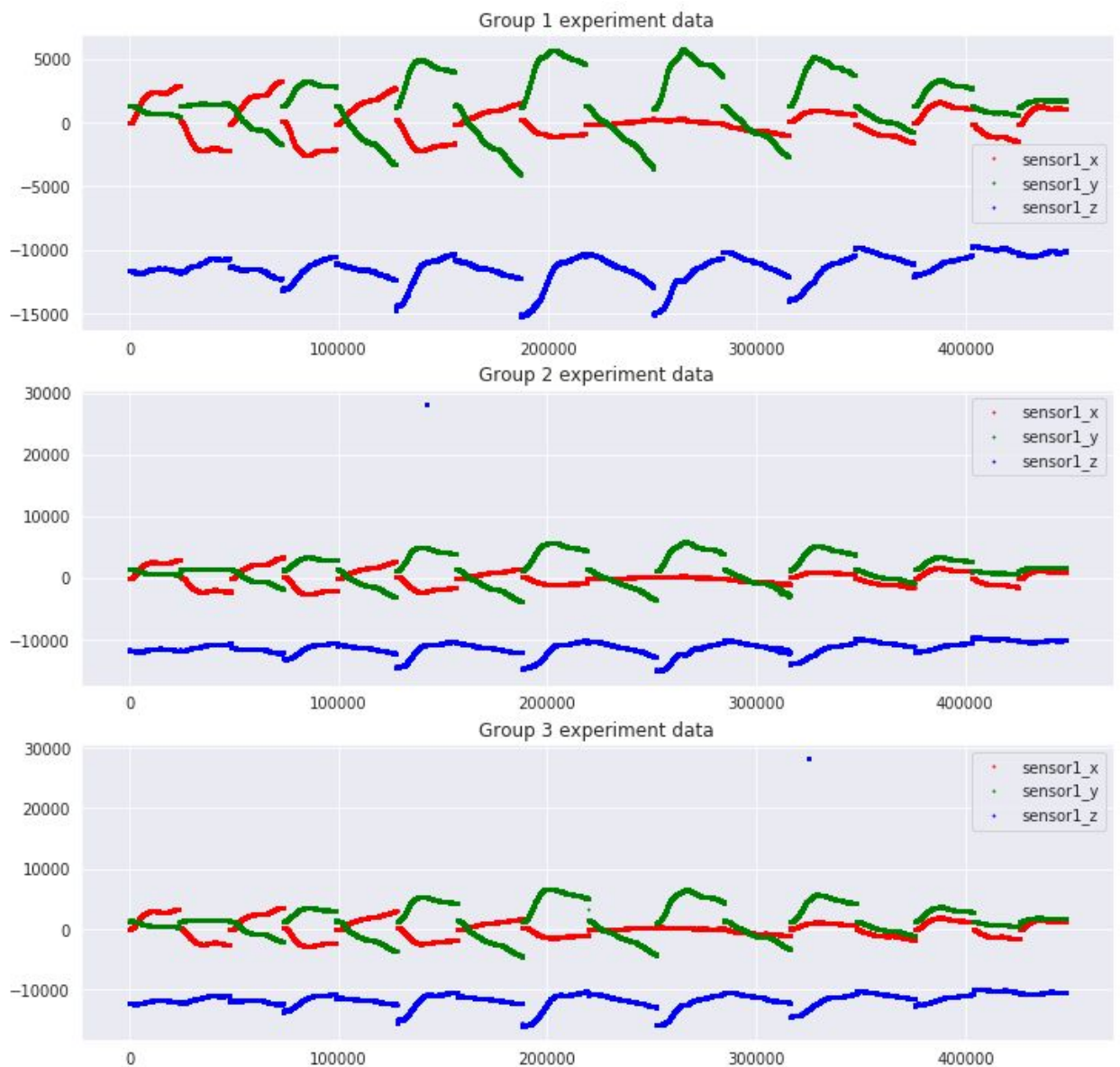
Note: The axis is defined in the pinky force sensor link.

### Global transformation calibration

After analyzing the collected data, we found the normal force changes in a large range when the force sensor does not have any movement in its vertical direction. Therefore, the problem may arise because the frame of ATI does not align perfectly with the force sensor frame.

1. Verify the repeatability of the experiments

Plot the raw force data and sensor data. The results show that except for some outliers, most of the data are the same.



2. Two steps to calibrate transformation between robot frame to ati frame:
3. Quantitative result

Evaluation of predicted force in test set		
	R^2	RMSE
Force_x	0.990306	0.01775
Force_y	0.964646	0.03034
Force_z	0.900858	0.095691